Supplemental Material

Index

Supplemental Methods
- Patient Selection and MR-acquisition
- MRI Quality Check
- Recruitment of Healthy Volunteers
- Microbleed Anatomical Rating Scale (MARS) atlas
- Creation of Susceptibility Mask
- Details of DTI Processing
- Details of Statistical Analysis

Supplemental Results
- Residuals of Linear Regression between Microbleeds and MD_z, Research Questions 1 and 2
- Residuals of Linear Regression between GCS and MD_z, Research Questions 2
- Associations between Microbleed Concentration and FA within Regions (Supplement to Research Question 1)
- Associations between Microbleed Concentration and FA in Connected Regions (Supplement to Research Question 2)

Supplemental Tables

Supplemental Figures

References of Supplemental Material

Supplemental Methods

Patient Selection and MR-acquisition

All 211 consecutive ≥18-year-old patients having sustained a moderate or severe TBI ≤24 hours before presenting at our level I trauma center emergency department were prospectively screened for the exclusion criteria specified in Figure A1. 197 patients or their next of kin were approached for informed consent. 120 gave informed consent and were invited for an MRI, which was unfeasible for 60 patients. The remaining 60 patients were scheduled for a standardized trauma protocol on a single 3T-MRI scanner (Magnetom Trio, Siemens Healthineers, Erlangen, Germany) 4.4 (2.0-5.3) and 27.1 (25.0-28.0) weeks after TBI. Table A1 summarizes the parameters of the relevant sequences. After the first MRI, 7 patients were lost to follow-up. After completing both MRI's, patients were excluded if they-showed severe non-traumatic cerebral pathology or if the image quality was poor. Additional patients had to be excluded as the scanning protocol had not been adhered to, or SWI data were lost from the scanner (Figure A1). This yielded 31 patients with SWI, DTI and T1WI data, obtained 3 (2-5) and 26 (25-28) weeks after TBI. Patient characteristics are summarized in Table A2.

MRI Quality Check

We checked the quality of SWI and T1-weighted images visually, and of the DTI acquisitions quantitatively using motion quantification, global and local signal losses detections, tensor model residuals and spatial distribution of principal diffusion axis. DTI to T1 registration, SWI to T1 registration and MARS-atlas and ICBM-DTI-81-atlas to T1 registration were visually inspected.

Recruitment of Healthy Volunteers

We recruited 28 volunteers using flyers and personal networks. 18-to-65-years-old people without a history of neurologic disease were eligible. Exclusion criteria were incomplete scanning protocol (N=1), poor image quality (N=2), evidence of significant brain abnormalities on conventional MRI-sequences (N= 1), and ≥1 definite microbleed (N=0)). The 24 finally included healthy volunteers were median 30.2 (IQR 22.6-52.4) years old. 16 (67%) were men.

Microbleed Anatomical Rating Scale (MARS) Atlas

In order to localize each microbleed or concomitant injury, we manually segmented the standard brain in Montreal Neurological Institute (MNI) space[1,2] into the regions specified in the MARS scoring template[3]. We compounded putamen, globus pallidus and nucleus caudatus into the region 'basal ganglia' (Figure A3). We defined the following compound regions: 1. cerebral hemispheres (frontal, parietal, temporal, occipital, insula) (left, right, and bilateral); 2. central brain region (deep and periventricular white matter, corpus callosum, putamen, globus pallidus, nucleus caudatus, thalamus, internal capsule, external capsule, brainstem, cerebellum)[4]; and 3. structures connected through the corpus callosum (frontal, parietal, temporal, occipital, deep and periventricular white matter, insula)[5,6].

Microbleed Evaluation

A Computer-Aided Detection (CAD)-system, described previously[7], evaluated the scans obtained at *t1* and *t2*, separately. Blinded for the other time-point, AE (neuroradiologist, 7 years of experience) classified each CAD-proposed microbleed as no, possible or definite microbleed, deciding on CAD-detections with the slightest doubt in consensus meetings with BG (neuroradiologist, 33 years of experience). Through visual screening, we manually added definite microbleeds missed by the CAD-system to the data set. Then each definite or possible microbleed was automatically segmented using intensity-based volume-constrained region growing. Each microbleed was allocated to a MARS-region using the non-linear registration tool FNIRT[8,9].

Bilateral symmetric lesions in the basal ganglia were not recorded as microbleeds since these are most likely calcifications[10].

A random sample of thirty of the microbleeds and the false-positive CAD-detections, the classification of which AE in the *single-scan* evaluation step assumed to be unequivocal, was reviewed by BG. She agreed on all of them. This suggests that the assumption of unequivocality of the classification of this subset of microbleeds was justified.

Each microbleed was automatically segmented using an intensity-based volume-constrained region growing. Errors made in the automatic segmentation step were manually corrected by AE. Each microbleed was allocated to a MARS-region based on automatic registration of the segmentation with the MARS atlas, using the non-linear registration tool FNIRT[11,12]. Microbleeds located at a border were distributed over the involved MARS-regions in proportion to the segmentation's volume in the MARS-regions. Microbleeds allocated to MARS-regions vulnerable to misregistration, such as occipital and cerebellar, were reviewed for need of manual re-allocation. If these were re-allocated to more than one region, they were counted as evenly distributed, e.g. a microbleed at the occipito-temporal border was counted as .5 occipital microbleed and .5 temporal microbleed.

Creation of Susceptibility Mask

To rule out bias caused by the effect of susceptibility on DTI findings[13], we analyzed DTI in the normal-appearing white matter only. To achieve that, we created an SWI-based mask for each patient to eliminate with high sensitivity from our DTI measurements any potential source of susceptibility related to trauma and its clinical management. We automatically segmented the microbleeds at *t2* using intensity-based volume-constrained region growing. Then we used VCAST[14] using views in orthogonal planes to manually adjust where necessary the automatic segmentations of each definite or possible microbleed, and to annotate other intra- and extra-axial lesions in close contact with brain parenchyma, whether secondary to TBI or to neurosurgical intervention. To rule out any confounding by the effect of susceptibility on DTI, we slightly over-segmented these sources of susceptibility. After registration of the atlas and the

susceptibility mask with the DTI-scans, we visually checked whether each extra-axial lesion was correctly eliminated from the DTI measurements.

Details of DTI Processing

DTI images were preprocessed using FSL software (http://www.fmri.ox.ac.uk/fsl/). After correction of distortions due to Eddy currents, the diffusion tensor was estimated and the local MD was calculated for each voxel of the brain in each patient and healthy volunteer, thus generating MD maps. We then used nonlinear registration of susceptibility masks, MD maps, and Mori's white matter atlas[15] to T1-weighted images, as implemented in FSL software (FNIRT procedures). The MD values were then extracted in the following compound regions: 1. *corpus callosum* (composed of splenium, body and genu); 2. *cerebral hemispheres* (composed of sagittal stratum, superior longitudinal fasciculus, corona radiata) (left and right); 3. *central brain region* (composed of external capsule, posterior and anterior limb of internal capsule, cerebral peduncle, corpus callosum, anterior and posterior brainstem, middle cerebellar peduncle). Regional MD was then calculated for each patient and healthy volunteer as the averaged MD within each region, and the Z-score of MD of each region in each patient was calculated as described in 'DTI processing' in the core text of this paper.

Details of Statistical Analysis

MD_z was normally distributed over the patients (Kolmogorov-Smirnov test). Therefore, we used two-sample T-tests to test differences in MD_z between patients and healthy volunteers.
The microbleed concentrations were not normally distributed over the patients (Kolmogorov-Smirnov test), but as residuals of linear regression seem to be randomly distributed with a no-clear pattern (Figure A4), we used linear regression analyses to examine the relation between the microbleed concentration and MD_z, as specified in the Figure. To verify that linear regression was allowed to adjust for the microbleed concentration in the region of MD-measurement (Table A3, Model 2), and for GCS at the injury site (Table A3, Model 3), we verified that the residuals of linear regression with GCS seem to be randomly distributed with a no-clear pattern (Figure A5), and we excluded a significant co-linearity between the microbleed concentration in the corpus callosum and in the regions connected through the corpus callosum, as well as between the microbleed concentration in the cerebral hemispheres and in the central brain region (variable inflation factor 1.12 and1.58, respectively).
B_{cmb-nr} was calculated as $B_{cmb-conc}$ divided by the patients' median volume of the region under evaluation (cm^3).

Supplemental Results

At *t1*, the 31 patients had a total of 856 microbleeds (24 (14-35) per patient), anatomically distributed as shown in Table A4. MD_z at *t2* was higher in patients than in healthy volunteers (Table A4).

Figure A2 graphically illustrates the associations between microbleed concentrations and MD_z discussed in the core paper.

Residuals of Linear Regression between Microbleeds and MD_z, Research Questions 1 and 2
The residual plots of the univariable linear regression analyses performed to answer research questions 1 and 2 are presented in Figure A4. The residuals seem to be randomly distributed with a no-clear pattern, substantiating the use of linear regression analyses.

Residuals of Linear Regression between GCS and MD_z, Research Question 2
Figure A5 presents the residual plots of the univariable linear regression analyses using GCS at the injury site as the independent variable, and MD_z in the corpus callosum and the central brain region as the independent variables. The residuals seem to be randomly distributed with a no-clear pattern, substantiating the use of linear regression analyses to adjust the analyses in research question 2 for GCS.

Associations between Microbleed Concentration and FA within Regions (Supplement to Research Question 1)
Within none of the cerebral hemispheres, FA_z at *t2* was associated with the microbleed concentration at *t1* (Table A5). Within the central brain region, FA_z was negatively associated with the microbleed concentration (Table A5), though this association lost its significance after correction for gender, age, and time passed from TBI to DTI-acquisition (Table A5), and was not independent of GCS at the injury site (bivariable linear regression corrected for GCS: $B_{cmbconc}$ -24.611 (95%CI -51.531 to 2.309, p=.072)).

Associations between Microbleed Concentration and FA in Connected Regions (Supplement to Research Question 2)
FA_z in the corpus callosum at *t2* was negatively associated with the microbleed concentration in the structures connected through the corpus callosum at *t1* (Table A5), even after correction for the microbleed concentration in the corpus callosum itself (Table A6 (Model 2)). The 95%CIs of $B_{cmb-conc}$ in these two regions did not overlap (Table A6).

FA_z in the central brain region was negatively associated with the microbleed concentration at *t1* in the cerebral hemispheres (Table A5), even after correction for the microbleed concentration in the central brain region itself (Table A6 (Model 2)). The 95%CIs of $B_{cmb-conc}$ in these two regions showed a slight overlap (Table A6).

All of these associations were independent of GCS, gender, age, and time passed from TBI to DTI-acquisition (Table A5, Table A6 (Models 3 and 4)).

Supplemental Tables

Table A1: Imaging Parameters

	MPRAGE	SWI	DTI
TR (ms)	2300	27	11700
TE (ms)	2.98	20.0	102
TI (ms)	900		
Flip angle (degrees)	9	15	
Bandwidth (Hz/pixel)	240	120	2056
Slice thickness (mm)	1.0	1.0	2.0
Voxel-size (mm)	1.0 x 1.0 x 1.0	1.0 x 1.0 x 1.0	2.0 x 2.0 x 2.0
FOV (mm)	256	250	256
TA (minutes)	5:21	7:44	6:16
Dimension	3D	3D	3D
Diffusion directions			30
B value (mT/m)			1000

Note –TA: acquisition time

Table A2: Demographic and Clinical Characteristics of the Patients

Number of patients	31
Gender: male[a,b]	17 (54.8%)
Age (years)[c]	27.3 (21.4-46.4)
At arrival at ED	
GCS[c]	3 (3-9)
Severity of TBI[a]	
Severe	22 (71.0%)
Moderate	9 (29.0%)
ISS[c]	25 (19-34)
CT findings[a]	
Epidural hematoma	4 (12.9%)
Subdural hematoma	9 (29.0%)
Subarachnoid hemorrhage	16 (54.6%)
≥1 contusion or intraparenchymal hemorrhage	13 (41.9%)
Intraventricular hemorrhage	2 (6.5%)
Signs of elevated intracranial pressure[d]	12 (38.7%)
Midline shift >5 mm	3 (9.7%)
Marshall classification[a]:	
Diffuse injury I-II	20 (64.5%)
Diffuse injury III	8 (25.8%)
Diffuse injury IV	3 (9.7%)
Mass lesion	0 (0%)
Hospitalization (days)[c]	10 (4-26)
Time from TBI to MRI-acquisition (weeks)[c]	
t1	3 (2-5)
t2	26 (25-28)
GOS-E[c]	
t1	5 (3-6)
t2	6 (5-6)
t3	7 (6-8)

Note - [a]Values are numbers of patients (percentage of the patients). [b]Self- or next-of-kin-reported gender. [c]Values are medians (interquartile range). [d]Generalized or hemispheric edema with effacement of sulci, compressed ventricles or basal cisterns and midline shift>5 mm

TBI: Traumatic brain injury, Age: age at TBI, ED: emergency department, GCS: Glasgow Coma Scale score, ISS: Injury Severity Score, GOS-E: Glasgow Outcome Scale score-Extended version, *t1*: 3 (2-5) weeks after TBI, *t2*: 26 (25-28) weeks after TBI, *t3*: 53.0 (51-56) weeks after TBI

Table A3: Exploration of Possible Confounders in Research question 2

Regression model	Variable	Research question 2.A	Research question 2.B
Model 1	Region 1	44.2 (23.6-64.8, .000)***	24.2 (6.8-41.5, .008)**
Model 2	Region 1	48.6 (27.1-70.2, .000)***	29.1 (7.1-51.1, .011)*
	Region 2	-3.5 (-9.1-2.0, .204)	-7.0 (-26.1-12.0, .455)
Model 3	Region 1	48.2 (26.6-70.1, .000)***	28.5 (10.0-46.5, .004)**
	GCS	.06 (-.05-.16, .291)	.06 (-.03-.14, .188)
Model 4	Region 1	52.9 (26.5-79.3, .000)***	29.1 2.2-56.0, .035)*
	Other variables with p<.05^A	none	none

Note – Results of uni-, bi- and multivariable linear regression analyses between microbleed concentration and MD_z in Functionally Connected Regions.

Research question 2.A: Is the microbleed concentration in the structures connected through the corpus callosum at *t1* associated with integrity of the corpus callosum at *t2*?
Research question 2.B: Is the microbleed concentration in the cerebral hemispheres at *t1* associated with white matter integrity in the central brain region at *t2*?

Numbers represent linear regression coefficient (95%CI, p). For Regions 1 and 2 this is $B_{cmb-conc}$: linear regression coefficient with microbleed concentration as independent variable.

Region 1: Structures connected through corpus callosum in research question 2.A, Cerebral hemispheres in research question 2.B
Region 2: Corpus callosum in research question 2.A, Central brain region in research question 2.B
Model 1: Univariable linear regression using the microbleed concentration in Region 1 as the independent variable, and MD_z in Region 2 as the dependent variable
Model 2: Bi-variable linear regression using the microbleed concentrations in Region 1 and in Region 2 as the independent variables, and MD_z in Region 2 as the dependent variable
Model 3: Bi-variable linear regression using the microbleed concentration in Region 1 and GCS at the injury site as the independent variables, and MD_z in Region 2 as the dependent variable
Model 4: Multivariable linear regression using the microbleed concentrations in Region 1 and in Region 2, gender, age at the day of DTI-imaging (years), and time passed from TBI to DTI-acquisition (weeks) as the independent variables, and MD_z in Region 2 as the dependent variable

[A] All variables other than microbleed concentration in region 1, which are associated with MD_z with p<0.05 in these multivariable analyses, are presented in this column
* p<.05, ** p<.01, *** p<.001

Table A4: Distribution of Microbleeds at *t1* and Distribution of MD$_z$ at *t2*

Region	Definite microbleeds (number)	MD$_z$ (SD)	
	Patients (*t1*)	Patients (*t2*)	Healthy volunteers
Cerebral hemispheres:			
Left	325.4 (8.8)	1.47 (.26-2.57)	.23 (-.82-.71)
Right	350.6 (7.8)	1.40 (.55-2.62)	-.05 (-.57-.64)
Both	675.9 (19.1)	1.45 (.31-2.62)	-.15 (-.71-.68)
Central brain region	170.3 (3.2)	.90 (.35-1.64)	.01 (-.32-.22)
Corpus callosum	39.9 (.0)	1.53 (.57-2.41)	-.15 (-.54-.32)
Structures connected through corpus callosum	700.9 (19.1)	NA	NA

Note – In each region p<.001 for difference in MD$_z$ between patients and healthy volunteers.

Values are expressed as total number of microbleeds (median number of microbleeds per person) and as median MD$_z$ (interquartile range). Numbers of microbleeds are not presented for the healthy volunteers, as due to the selection criteria, none of the healthy volunteers had any microbleed by definition

t1: 3 (2-5) weeks after TBI. *t2*: 26 (25-28) weeks after TBI. MD$_z$: Z-score of mean diffusivity. SD: standard deviation. NA: not assessed, as MD$_z$ in this region is not part of the research questions.

Table A5: Association between Microbleed Concentrations at *t1* and FA$_z$ at *t2*

Research question	Region of microbleed-concentration	White matter region of FA measurement	Univariable $B_{cmb\text{-}conc}$ (95%CI)	p	Multivariable[A] $B_{cmb\text{-}conc}$ (95%CI)	p
1.a	Cerebral hemispheres: Left	Cerebral hemispheres: Left	-19.798 (-43.203 to 3.607)	.094	-24.358 (-53.120 to 4.403)	.094
	Right	Right	-7.318 (-25.315 to 10.678)	.412	-9.254 (-31.565 to 13.058)	.402
1.b	Central brain region	Central brain region	-26.205 (-51.044 to -1.365)	.039	-21.810 (-48.472 to 4.853)	.105
2.a	Structures connected through the corpus callosum	Corpus callosum	-84.066 (-111.113 to -57.019)	.000	-87.749 (-122.441 to -53.058)	.000
2.b	Cerebral hemispheres	Central brain region	-52.38 (-76.053 to -28.713)	.000	-52.292 (-83.443 to -21.141)	.002

Note – Results of linear regression analyses. None of the variables other than microbleed concentration is associated with FA$_z$ with p<.05 in the multivariable analyses.

FA$_z$: Z-score of fractional anisotropy. *t1*: 3 (2-5) weeks after trauma. *t2*: 26 (25-28) weeks after trauma. $B_{cmb\text{-}conc}$: linear regression coefficient with microbleed-concentration as independent variable. $B_{cmb\text{-}nr}$: linear regression coefficient with number of microbleeds as independent variable.
[A]Multivariable linear regression analyses with the following independent variables: microbleed concentration, gender, age at the day of DTI-imaging (years), and time passed from TBI to DTI-acquisition (weeks)

Table A6: Exploration of Possible Confounders in Research question 2, analyses on FA_z

Regression model	Variable	Research question 2.A	Research question 2.B
Model 1	Region 1	-84.066 (-111.113 to -57.019, .000)***	-52.383 (-76.053 to -28.713, .000)***
Model 2	Region 1	-86.828 (-115.791 to -57.866, .000)***	-53.786 (-84.103 to -23.469, .001)**
	Region 2	2.205 (-5.304 to 9.714, .552)	2.003 (-24.233 to 28.240, .877)
Model 3	Region 1	-84.043 (-113.427 to -54.659, .000)***	-53.420 (-79.054 to -27.785, .000)***
	GCS	.000 (-1.39 to .140, .996)	-.014 (-.135 to .106, .810)
Model 4	Region 1	-89.742 (-126.434 to -53.049, .000)***	-52.579 (-91.169 to -13.990, .010)*
	Other variables with p<.05[A]	none	none

Note – Results of uni-, bi- and multivariable linear regression analyses between microbleed concentration and FA_z in Functionally Connected Regions.

Research question 2.A: Is the microbleed concentration in the structures connected through the corpus callosum at *t1* associated with integrity of the corpus callosum at *t2*?
Research question 2.B: Is the microbleed concentration in the cerebral hemispheres at *t1* associated with white matter integrity in the central brain region at *t2*?

Numbers represent linear regression coefficient (95%CI, p). For Regions 1 and 2 this is $B_{cmb-conc}$: linear regression coefficient with microbleed concentration as independent variable.

Region 1: Structures connected through corpus callosum in research question 2.A, Cerebral hemispheres in research question 2.B
Region 2: Corpus callosum in research question 2.A, Central brain region in research question 2.B
Model 1: Univariable linear regression using the microbleed concentration in Region 1 as the independent variable, and FA_z in Region 2 as the dependent variable
Model 2: Bi-variable linear regression using the microbleed concentrations in Region 1 and in Region 2 as the independent variables, and FA_z in Region 2 as the dependent variable

Model 3: Bi-variable linear regression using the microbleed concentration in Region 1 and GCS at the injury site as the independent variables, and FA_z in Region 2 as the dependent variable

Model 4: Multivariable linear regression using the microbleed concentrations in Region 1 and in Region 2, gender, age at the day of DTI-imaging (years), and time passed from TBI to DTI-acquisition (weeks) as the independent variables, and FA_z in Region 2 as the dependent variable

[A] All variables other than microbleed concentration in region 1, which are associated with FA_z with $p<0.05$ in these multivariable analyses, are presented in this column

* $p<.05$, ** $p<.01$, *** $p<.001$

Supplemental Figures
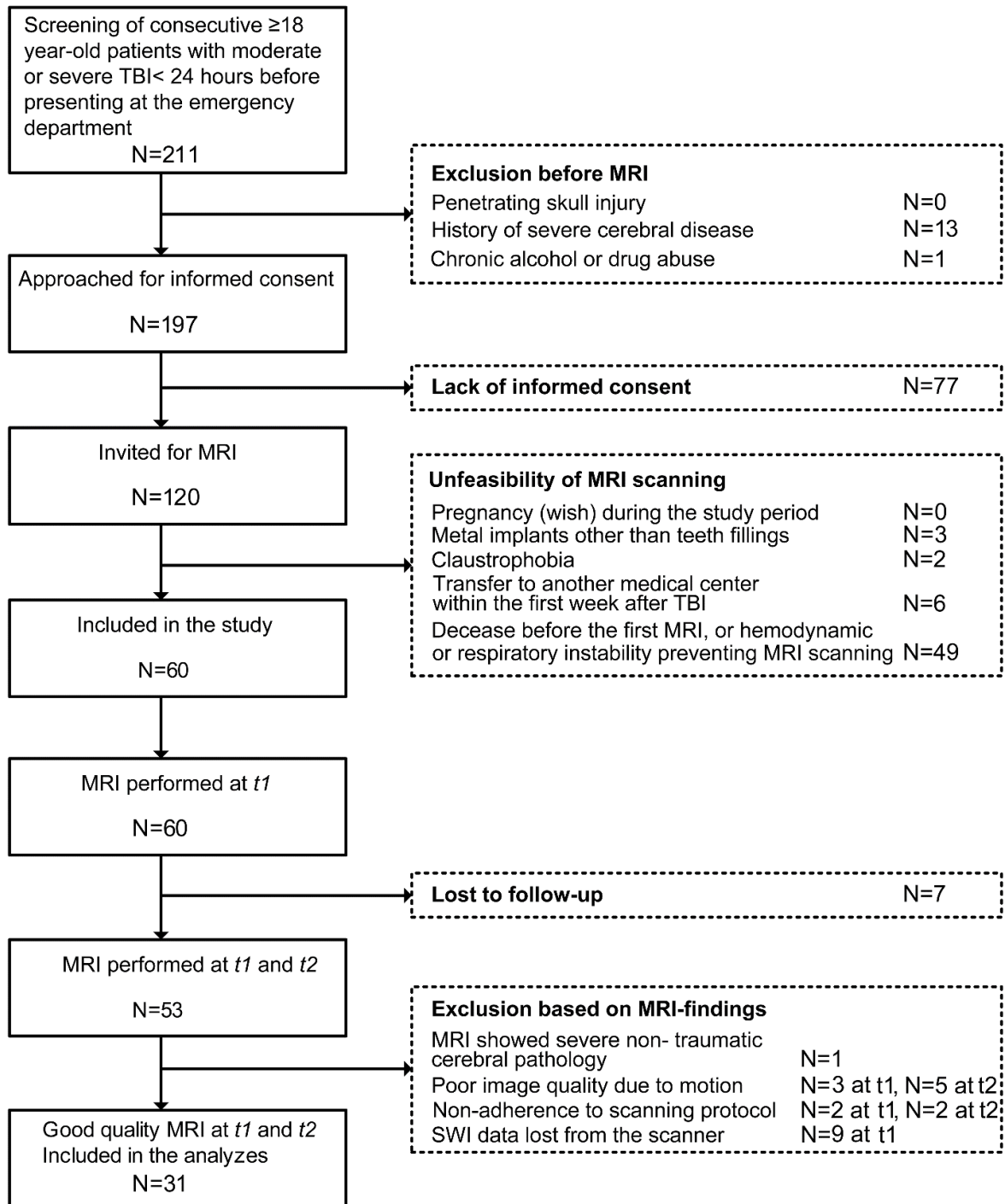
Figure A1: Patient Selection Flowchart

Selection procedure starting with all consecutive ≥18-year-old patients who were screened prospectively if they had sustained a moderate or severe TBI less than 24 hours before presenting at our emergency department. The exclusion criteria are specified in the boxes in the right part of this flowchart. Numbers represent numbers of patients
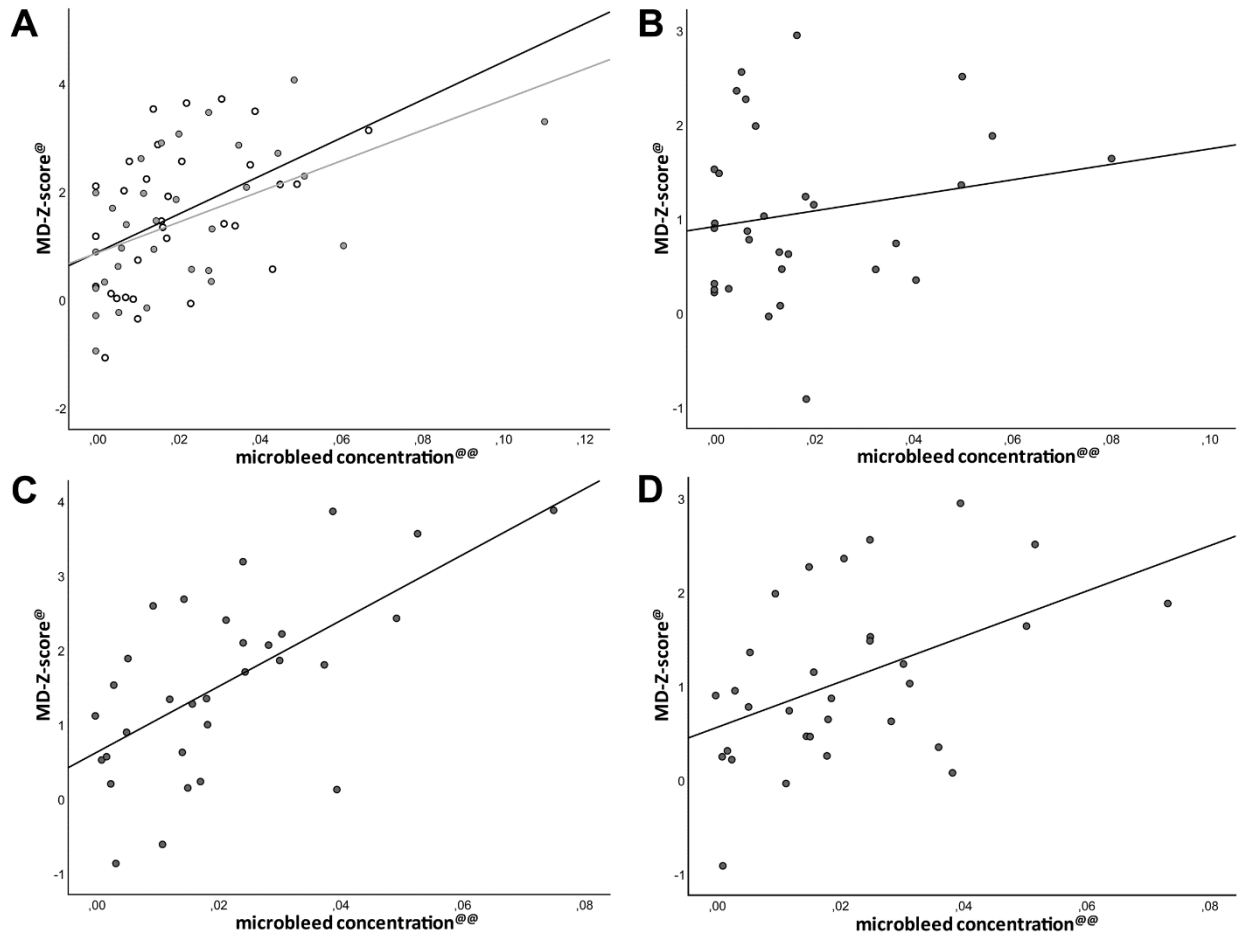
Figure A2: Results of Linear Regression

A. Relation between the microbleed concentration at *t1* and MD_z at *t2* within the cerebral hemispheres (research question 1.A). Grey circles represent the right hemisphere, open circles represent the left hemisphere.

B. Relation between the microbleed concentration at *t1* and MD_z at *t2* within the central brain structures (research question 1.B).

C. Relation between microbleed concentration at *t1* in structures connected through the corpus callosum and MD_z at *t2* in the corpus callosum (research question 2.A).

D. Relation between microbleed concentration at *t1* in the cerebral hemispheres and MD_z at *t2* in the central brain region (research question 2.B).

Note: @: Z-score of mean diffusivity. @@: (number of microbleeds) / (volume (cm^3) on the patient's T1-weighted scan at *t1*). Lines are linear regression lines
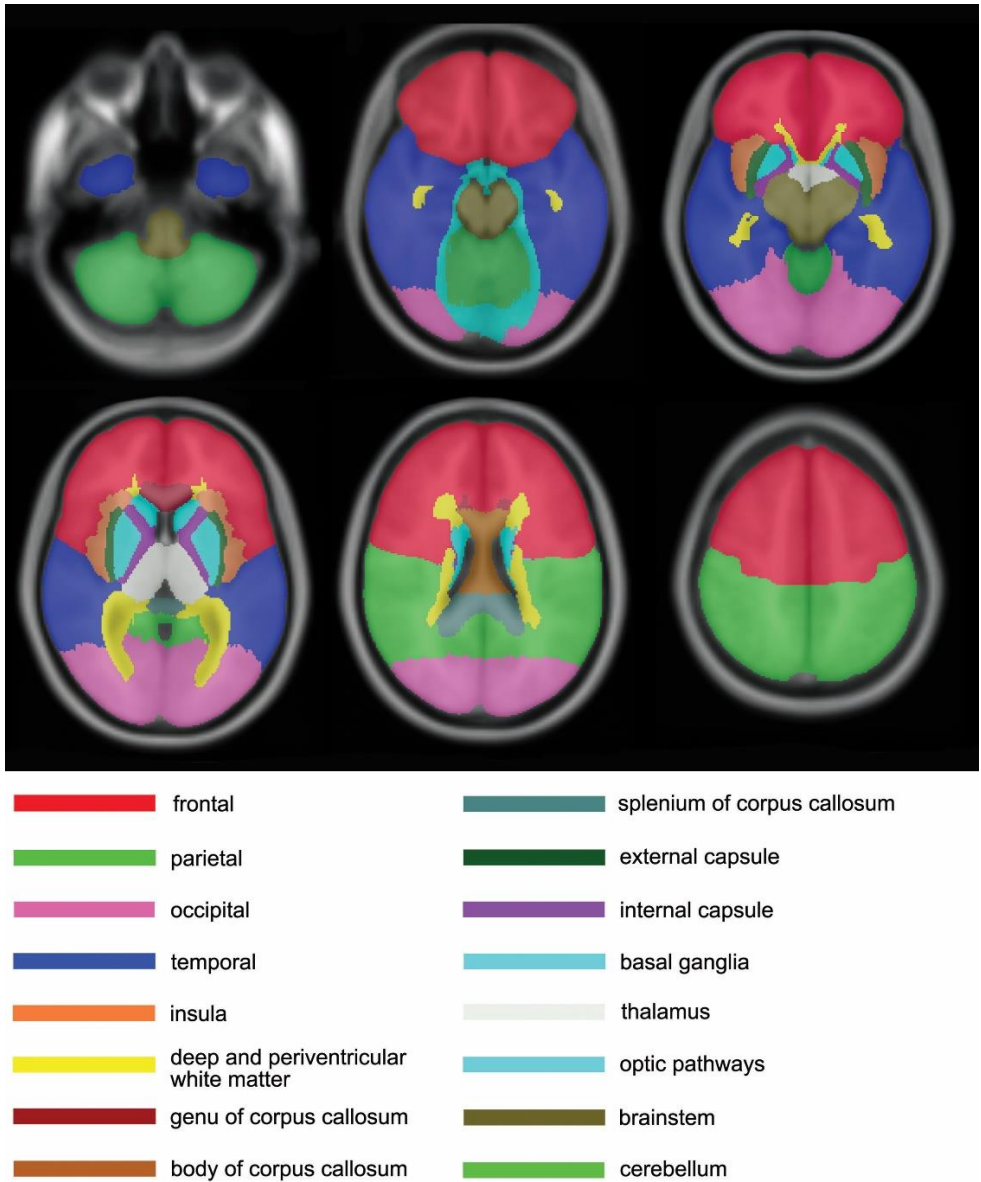
Figure A3: Manually Segmented Anatomical Regions Specified in the MARS Scoring Template

Manually segmented regions for evaluation of the anatomical distribution of microbleeds over the brain. The regions specified in the MARS scoring template[3] are color-coded and superimposed on the background images representing the standard brain in MNI-space.

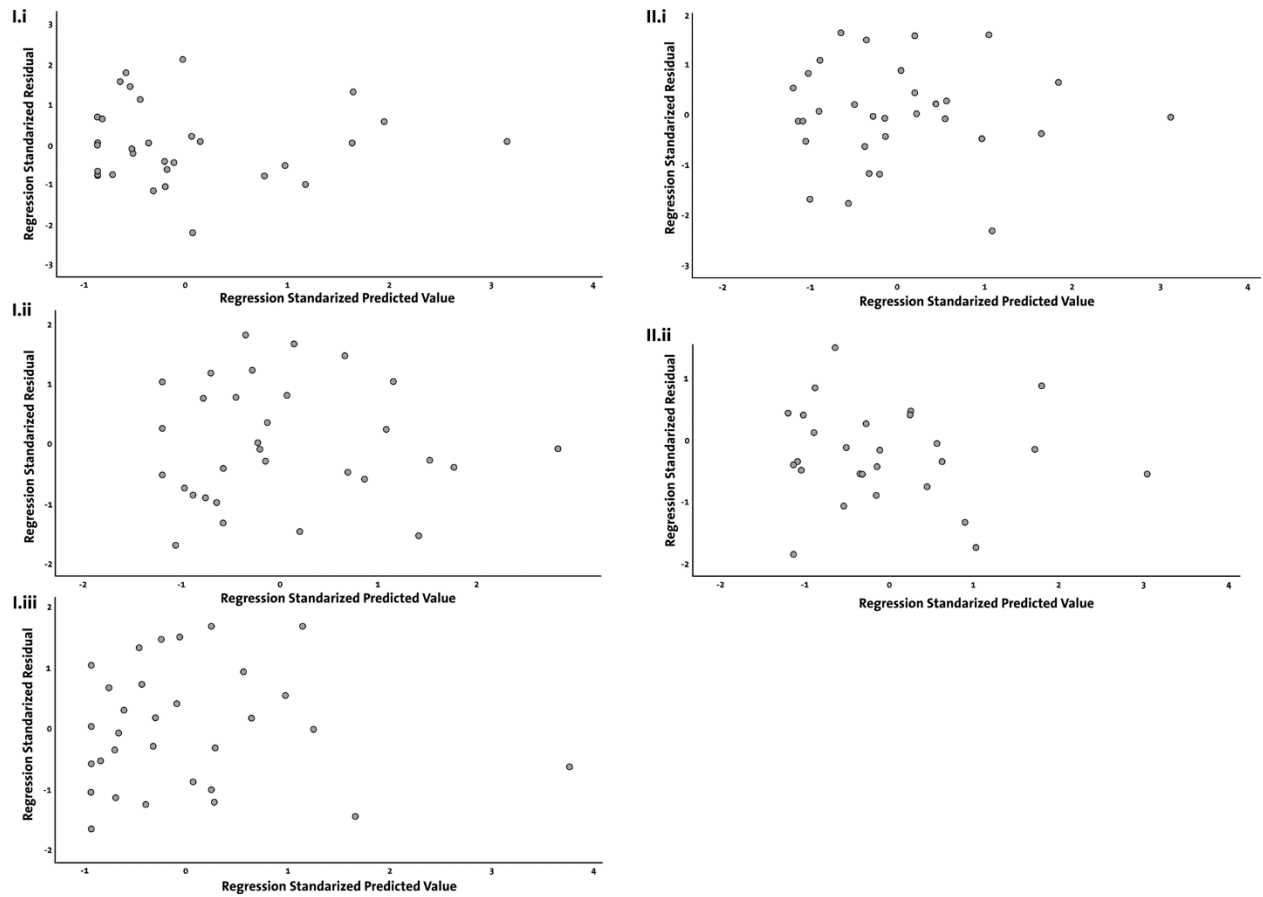MARS: Microbleed anatomical rating scale, MNI: Montreal Neurological Institute

Figure A4: Residual Plots for Linear Regression, Research Questions 1 and 2
I. Residual plot for regression between the microbleed concentration at *t1* and MD$_z$ at *t2* within the central brain structures (I.i) and within the cerebral hemispheres (I.ii: left; I.iii: right hemisphere).
II. Residual plot for regression between microbleed concentration at *t1* in structures connected through corpus callosum and MD$_z$ at *t2* in the corpus callosum (II.i) and between microbleed concentration at *t1* in the cerebral hemispheres and MD$_z$ at *t2* in the central brain region (II.ii)
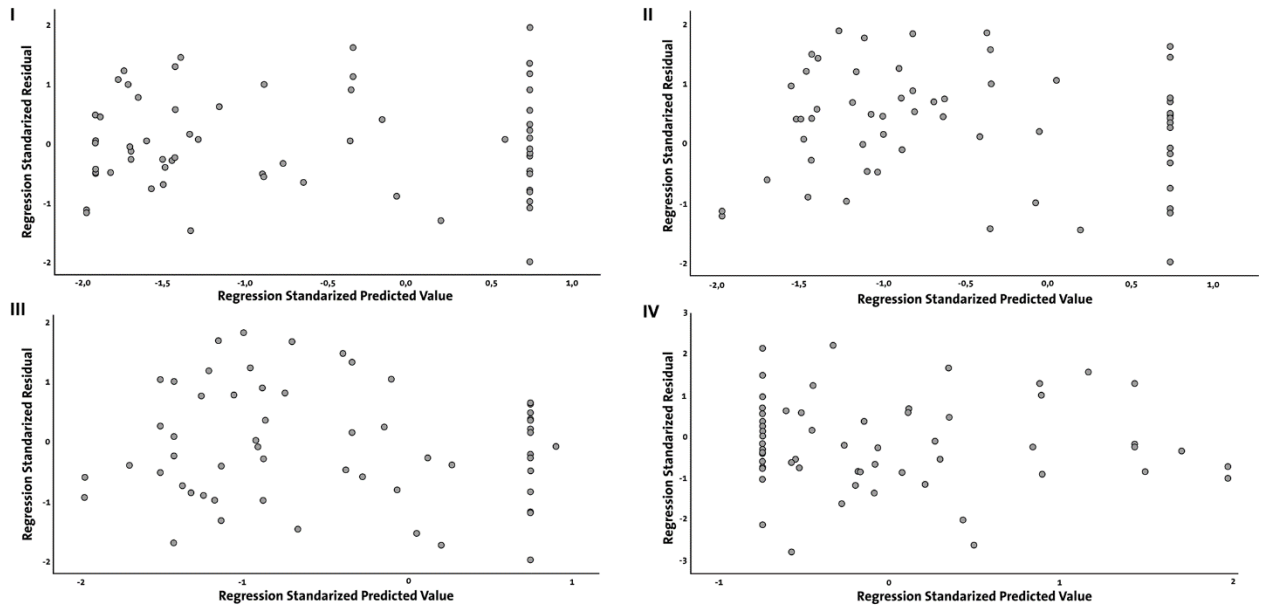
Figure A5: Residuals Plots for Linear Regression between GCS and MD$_z$

Residual plot for regression between GCS at the injury site and MD$_z$ in the right (I) and left cerebral hemisphere (II), in the corpus callosum (III), and the central brain region (IV)

References of Supplemental Material

1. MNI ICBM 152 non-linear 6th Generation Symmetric Average Brain Stereotaxic Registration Model. http://nist.mni.mcgill.ca/?p=858. Accessed December 2017.

2. Grabner G, Janke AL, Budge MM, et al. Symmetric atlasing and model based segmentation: an application to the hippocampus in older adults. In: Larsen R, Nielsen M, Sporring J (eds). Medical Image Computing and Computer-Assisted Intervention – MICCAI 2006. MICCAI 2006. Lecture Notes in Computer Science, vol 4191. Springer, Berlin; 2006

3. Gregoire SM, Chaudhary UJ, Brown MM, et al. The Microbleed Anatomical Rating Scale (MARS): reliability of a tool to map brain microbleeds. Neurology 2009;21:1759–1766. doi: 10.1212/WNL.0b013e3181c34a7d

4. AW van der Eerden, O Khalilzadeh, V Perlbarg, et al. White matter changes in comatose survivors of anoxic ischemic encephalopathy and traumatic brain injury: comparative diffusion tensor imaging study. Radiology 2014;270(2):506-516. doi: 10.1148/radiol.13122720

5. Oishi K, Faria AV, Van Zijl PCM, et al. MRI Atlas of Human White Matter, 2nd ed. London, UK: Academic Press, 2010

6. Schmahmann JD, Pandya DN. Fiber pathways of the brain, 1st ed. New York, NY: Oxford University Press, 2006

7. Van den Heuvel TL, van der Eerden AW, Manniesing R, et al. Automated detection of cerebral microbleeds in patients with traumatic brain injury. *Neuroimage Clin* 2016;12:241-51

8. FSL FNIRT. https://fsl.fmrib.ox.ac.uk/fsl/fslwiki/FNIRT Accessed December, 2017

9. Jenkinson M, Beckmann CF, Behrens TE, et al. FSL. *Neuroimage* 2012;62(2):782-90

10. Tsushima Y, Endo K. Hypointensities in the brain on T2*-weighted gradient-echo magnetic resonance imaging. *Curr Probl Diagn Radiol* 2006;4:140–50

11. FSL FNIRT. https://fsl.fmrib.ox.ac.uk/fsl/fslwiki/FNIRT. Accessed December 2017.

12. Jenkinson M, Beckmann CF, Behrens TE, et al. FSL. *Neuroimage* 2012;62(2):782-90

13. Zhang J, Tao R, Liu C, et al. Possible effects of iron deposition on the measurement of DTI metrics in deep gray matter nuclei: an in vitro and in vivo study. Neurosci Lett 2013;551:47-52. doi: 10.1016/j.neulet.2013.07.003

14. van de Leemput SC, Meijer FJA, Prokop M, et al. Cerebral white matter, gray matter and cerebrospinal fluid segmentation in CT using VCAST: a volumetric cluster annotation and segmentation tool. European Congress of Radiology, 2017,1-10. http://www.diagnijmegen.nl/index.php/Publication?bibkey=Leem17

15. Mori S, Oishi K, Jiang H, et al. Stereotaxic white matter atlas based on diffusion tensor imaging in an ICBM template. Neuroimage 2008;40(2):570–582. doi: 10.1016/j.neuroimage.2007.12.035